

## Recombination in $\alpha$ -Si:H: Transitions through defect states

R. A. Street, D. K. Biegelsen and R. L. Weisfield  
*Xerox Palo Alto Research Center, Palo Alto, California 94304*

(Received 21 May 1984)

To obtain detailed information about recombination processes near room temperature in  $\alpha$ -Si:H we have measured the steady-state and transient response of luminescence, light-induced ESR, and photoconductivity in lightly doped and undoped samples. The low-energy luminescence is at a different energy in  $n$ - and  $p$ -type  $\alpha$ -Si:H, and has an intensity-dependent decay. The results lead us to propose a new model—that the radiative transition is the capture of a majority carrier into a neutral dangling bond, having a low radiative efficiency and only a small Stokes shift. Measurements of the quantum efficiency for generating light-induced ESR (or LESR) confirm that a transition through a dangling bond is the dominant recombination mechanism in all samples, and is predominately non-radiative. We discuss the trapping mechanism and conclude that a single multiphonon process does not seem possible. Instead we suggest that the mechanism may be a cascade through as yet unidentified excited states. Transient luminescence, LESR, and photoconductivity each show that the response time is much longer in doped samples than in undoped samples.

### I. INTRODUCTION

A great deal of information has been obtained about the recombination of excess carriers in  $\alpha$ -Si:H. The principal experiments used in these studies are luminescence,<sup>1</sup> light-induced ESR (LESR),<sup>2,3</sup> photoconductivity,<sup>4-7</sup> and induced absorption.<sup>8</sup> There are several recombination processes, both radiative and nonradiative, with the relative importance of each depending on the experimental conditions. Previous papers in this series have mostly explored the low-temperature mechanisms which are often dominated by a luminescence transition. This paper further investigates the high-temperature regime in which the recombination is predominately nonradiative. In particular, we compare undoped and doped samples and discuss the details of the recombination.

At low temperature the dominant recombination processes are a radiative tunneling transition between band-tail states and nonradiative tunneling to dangling-bond defects.<sup>1</sup> Surface and Auger recombination are present, but tend to be less important.<sup>1</sup> Some recent measurements also suggest another process of, as yet, unknown origin.<sup>9</sup> The low-temperature recombination is characterized by tunneling rather than extensive diffusion of carriers because the presence of a large density of band-tail states causes rapid trapping in states much deeper than  $kT$ .<sup>1</sup>

Near room temperature, carriers are more mobile so that carrier transport is an important factor in the recombination. The band-edge luminescence is strongly quenched, this effect being attributed to trapping at dangling bonds.<sup>1</sup> There is a second weak luminescence transition at lower energy that tends to dominate near 300 K and which has also been associated with recombination at the defects.<sup>10</sup> This band is seen particularly in doped samples in which the defect density is known to be high. The association of dangling bonds with recombination has

been confirmed recently by time-of-flight photoconductivity.<sup>11</sup> The capture rates of electrons and holes in undoped material and minority carriers in doped material have been measured by this technique. As we shall see, one of the problems addressed in this paper is to reconcile these rates with those obtained in other experiments.

The results of gap-cell photoconductivity are rather confusing since data from many groups do not seem to agree well.<sup>4-7</sup> In addition, surface and contact effects may complicate the results, and these have not been fully resolved.<sup>12,13</sup> Generally, the photoconductivity recombination is attributed to deep gap states although several alternative models have been suggested. The photoconductivity decay extends for a long time, particularly in doped samples, with a power-law behavior that has been attributed to dispersive transport.<sup>5</sup> The induced absorption similarly shows extended power-law decays, again associated with dispersive transport.<sup>8</sup> The origin of the absorption is believed to be band-tail holes in undoped  $\alpha$ -Si:H and defects in doped material.

To fully understand recombination, we need to find out which deep states are important and what transition mechanisms operate. This paper approaches these questions in three ways. First, we present new luminescence data aimed at a better understanding of the defect transition. Based on the results, we propose a new model which is substantially different from our previous ideas.<sup>10</sup> Second, we use LESR to identify the recombination centers, and show that, in doped material, dangling-bond transitions do indeed dominate. Third, we measure the recombination rates by observing the transient decay of luminescence, ESR, and gap-cell photoconductivity. These data show an apparent discrepancy with the time-of-flight results, the possible origins of which we discuss. In addition, we discuss the mechanisms of deep trapping and suggest that transitions through excited states might be important.

## II. LUMINESCENCE DATA

The sample-preparation procedure and the experimental techniques for measuring luminescence have been described elsewhere.<sup>14</sup> The excitation wavelength used was either 6471 Å (Kr<sup>+</sup> laser) or 1.06 μm [yttrium-aluminum-garnet (YAG) laser]. For the higher-energy excitation the absorption depth is about 1–2 μm, so that for these samples, all of which have a thickness of 5 μm or more, the light is completely absorbed. At 1.06 μm the absorption is weak and depends on the doping level of the samples, and this will be apparent in the results.

Figure 1 shows some examples of luminescence spectra of undoped and doped samples at 250 K, and Table I lists the relative intensities. The undoped sample has its main peak at 1.1 eV. This luminescence band has been identified as a transition between the band tails.<sup>1</sup> The transition occurs at ~1.4 eV at low temperature, but moves rapidly to low energy with increasing temperature.<sup>15</sup> The origin of this shift is believed to be that the shallow band-tail states are rapidly ionized and recombine nonradiatively. As we show below, between 250 and 300 K the band-tail luminescence continues to be strongly quenched and the luminescence becomes dominated by a second transition at 0.8–0.9 eV, which can be seen as a weak shoulder in the spectrum of Fig. 1.

Figure 1 also shows the effect of doping on the luminescence spectrum. Previous measurements at 10 K found that when the doping exceeds 100 ppm, the band-tail luminescence is quenched and replaced by a transition at about 0.9 eV.<sup>10</sup> Figure 1 shows that the sensitivity to doping is much greater at 250 K. In boron-doped samples, a doping level of 10 ppm is sufficient to quench the band-tail peak so that the spectrum is dominated by a

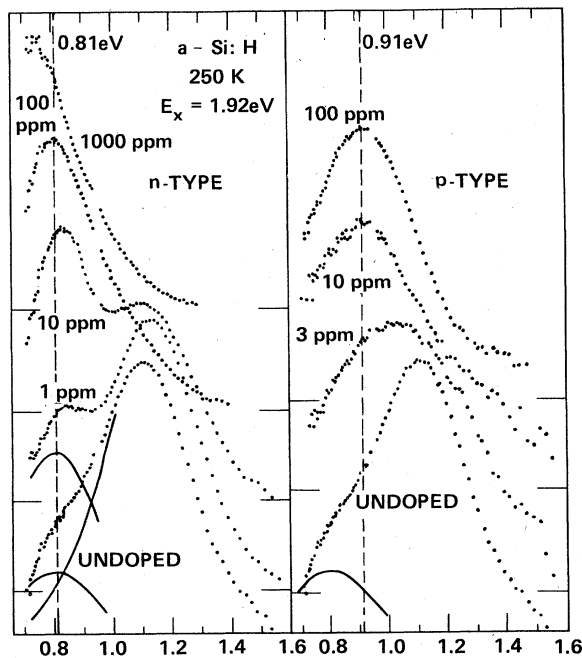


FIG. 1. Luminescence spectra of doped and undoped *a*-Si:H measured at 250 K, showing the band-tail line at 1.1 eV and the two defect peaks at 0.81 and 0.91 eV.

TABLE I. Relative intensities of the luminescence bands in doped and undoped *a*-Si:H at 250 K. The  $D_P$  peak is at 0.81 eV, the  $D_B$  peak is at 0.91 eV, and the band-tail peak is at 1.1 eV. Doping levels are given by the gas-phase concentration.

Doping level	$D_P$	$D_B$	Band tail
$10^{-6}$ PH <sub>3</sub>		5.3	10.0
$10^{-5}$ PH <sub>3</sub>		9.2	6.7
$10^{-4}$ PH <sub>3</sub>		14.2	<1
$10^{-3}$ PH <sub>3</sub>		6.5	<0.5
$3 \times 10^{-6}$ B <sub>2</sub> H <sub>6</sub>	1.1		1.1
$10^{-5}$ B <sub>2</sub> H <sub>6</sub>	1.9		~0.5
$3 \times 10^{-5}$ B <sub>2</sub> H <sub>6</sub>	2.5		<0.5
$10^{-4}$ B <sub>2</sub> H <sub>6</sub>	3.5		<0.8
Undoped (1)		1.4	6.6
Undoped (2)		2.1	2.4

transition at 0.91 eV, which we denote the  $D_B$  peak (since this luminescence has been associated with defect states). The sample doped with 3 ppm has a broader spectrum, indicating the presence of both peaks. Increasing the boron doping leads to a weak increase in the intensity of the  $D_B$  peak.

The relative intensities of the two luminescence transitions are excitation-intensity dependent. The band-tail luminescence increases superlinearly with intensity, in agreement with previous data,<sup>16</sup> whereas the  $D_B$  peak is linear, at least over one order of magnitude change in intensity. Hence, measurement at lower intensity than in Fig. 1 shows an even more pronounced quenching of the band-tail peak with doping.

Phosphorus doping is qualitatively similar in that doping quenches the band-tail peak and replaces it with one at lower energy. However, there are some significant differences. First, a larger doping level is required to quench the 1.1-eV peak, which is clearly visible at 10 ppm. In fact, it seems that light doping at first increases the intensity of this transition (see Table I). Second, the defect transition is at a different energy, 0.81 eV, and also has a narrower linewidth. We therefore denote it by  $D_P$ , as a separate transition. The peak energy decreases at the highest doping level, which we believe is probably due to a decrease in the band gap. Third, the defect luminescence intensity is larger in *n*-type samples than in *p*-type samples by a factor of about 4.

Figure 2 shows luminescence spectra of the same undoped sample at 275 K and room temperature. The band-tail peak is the more strongly quenched, so that at room temperature the defect peak at 0.8 eV dominates. This transition is very similar in position and line shape to the  $D_P$  peak, as can be seen by the spectrum of the 100-ppm-doped sample in Fig. 2. However, the intensity is 5–10 times weaker than that found in the doped sample.

We have also measured the luminescence spectra using 1.06-μm excitation. Previous experiments at 10 K found that subgap excitation quenched the band-tail luminescence but not the defect transition.<sup>10</sup> We observe this effect also at 250 K. The luminescence line shape of the defect is not noticeably changed, and the luminescence efficiency, when corrected for the low absorption, is simi-

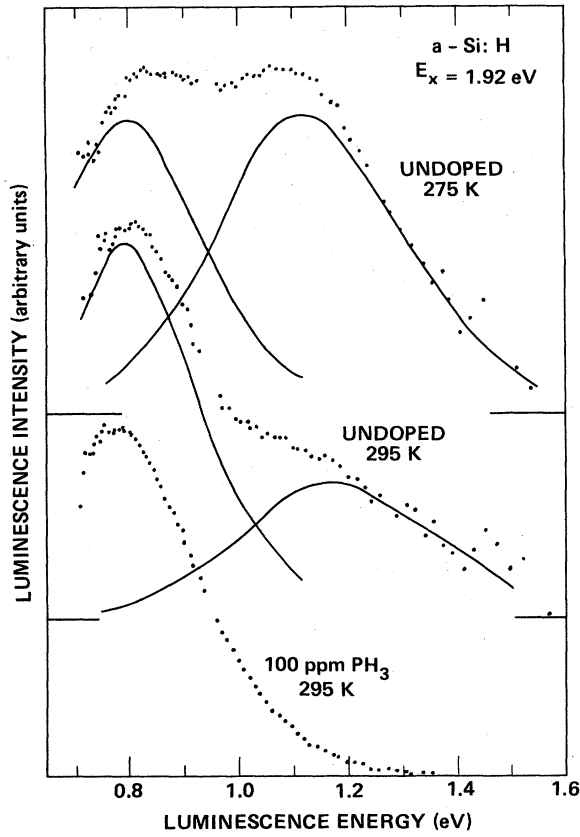


FIG. 2. Luminescence spectra of an undoped sample at 275 and 295 K compared with an  $n$ -type sample. Solid lines are a deconvolution into two peaks.

lar to that found with above-gap excitation. Since the absorption increases with doping,<sup>17</sup> the observed luminescence intensity changes much more than shown in Table I. For both excitation energies the quantum efficiency is low,  $<1\%$ , and the luminescence intensity is proportional to the excitation intensity over at least an order of magni-

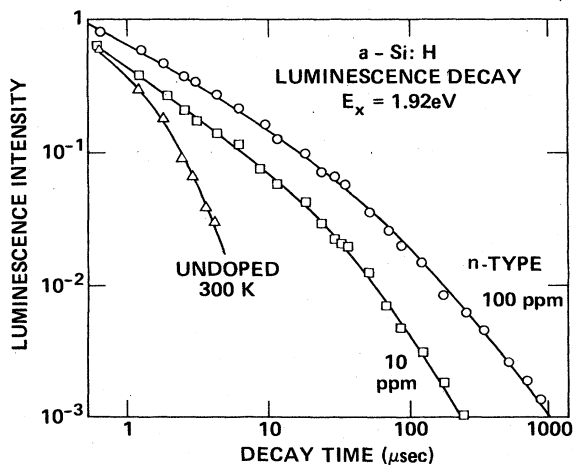


FIG. 3. Luminescence decay of the defect transition after a short ( $\sim 1 \mu\text{sec}$ ) excitation pulse for  $n$ -type samples at 250 K and an undoped sample at 300 K.

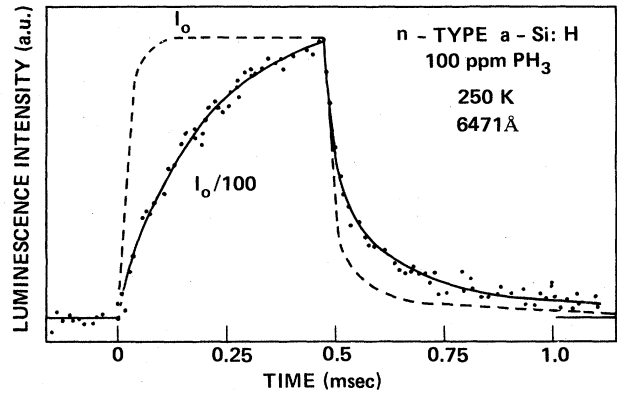


FIG. 4. Example of the rise and decay of the 0.81-eV luminescence band in  $n$ -type  $\alpha$ -Si:H for two excitation intensities differing by a factor of 100. For clarity, only one set of data points is shown.

tude change.

Further information about the recombination is obtained from the transient luminescence response, examples of which are shown in Figs. 3–5, which illustrate the effects in different ways. Only data from  $n$ -type samples are shown, since the  $p$ -type samples show qualitatively the same behavior. The decay times for the defect peak at 250 K increase with doping level (Fig. 3), and at a phosphorus doping level of 100 ppm the decay is observable to 1 msec. The results are typical for a broad distribution of decay times extending more than three decades.<sup>15</sup> Boron doping is similar, although the decay times are generally about a factor of 2 less. However, the decay of the defect peak in undoped samples is very much faster, as shown in Fig. 3. These data are in fact measured at 300 K to reduce the effect of the band-tail peak, but the results are comparable because the temperature dependence is weak.

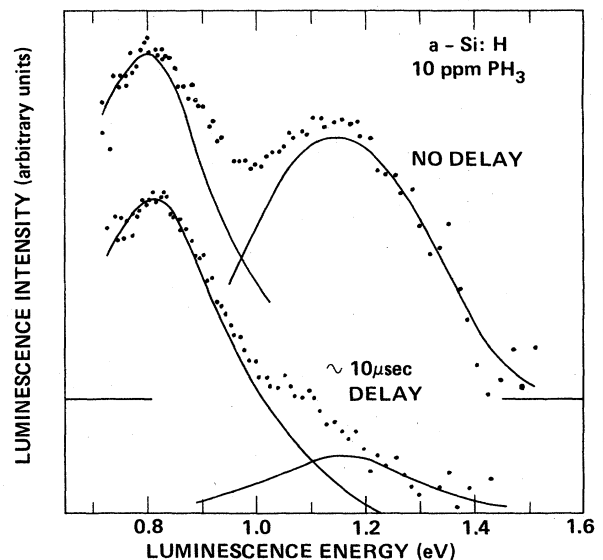


FIG. 5. Time-resolved luminescence spectra of an  $n$ -type sample showing the rapid quenching of the band-tail peak compared to the defect transition.

The rise and decay times are intensity dependent, decreasing as the excitation intensity increases, as shown in Fig. 4. The recombination is therefore indicative of bimolecular kinetics. The use of a long excitation pulse of weak intensity enhances the long-decay components, as is seen by comparing Figs. 3 and 4. Another feature of the transient luminescence is that the decay of the band-tail peak is much faster than that of the  $D_B$  or  $D_P$  peaks. This can be seen most easily in time-resolved spectra, an example of which is shown in Fig. 5 for an  $n$ -type sample. Finally, transient measurements have also been made with subgap excitation and have been found to have the same characteristics, particularly the same dependence on doping and intensity.

### III. LIGHT-INDUCED ESR

Light-induced ESR measurements can, in principle, provide the identification of the states involved in recombination. Past LESR data have demonstrated that the optically excited states in  $n$ -type  $a$ -Si:H are neutral dangling bonds and band-tail electrons (band-tail holes in  $p$ -type material).<sup>18</sup> In undoped samples, band-tail electrons and holes are observed together. The decay of LESR measures the recombination rate of these light-induced states; some examples are shown in Fig. 6. Just as for the luminescence, we observe that the doped samples (both  $n$  and  $p$  type) have a longer decay time than the undoped samples. The undoped sample could not be measured above 220 K because of its low LESR spin density due to the faster recombination. The LESR decay of the  $n$ -type sample extends up to 0.1 sec, which is apparently a longer time constant than the luminescence. Note, however, that LESR measures the number of excited carriers,  $N$ , whereas luminescence measures  $dN/dt$ . The result is the same only in the case of an exponential decay. In the present case the decay more closely resembles a power law, so that the luminescence is expected to decrease more rapidly. Taking this difference into account, we believe that the two experiments measure comparable response times, although precise agreement is hard to determine because of the broad distributions in the decay times.

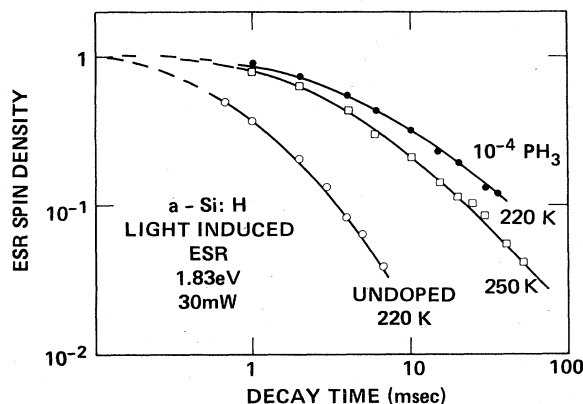


FIG. 6. Decay of light-induced ESR at 220 and 250 K, showing the faster response of undoped samples. The power density is approximately the same as that for the luminescence decay.

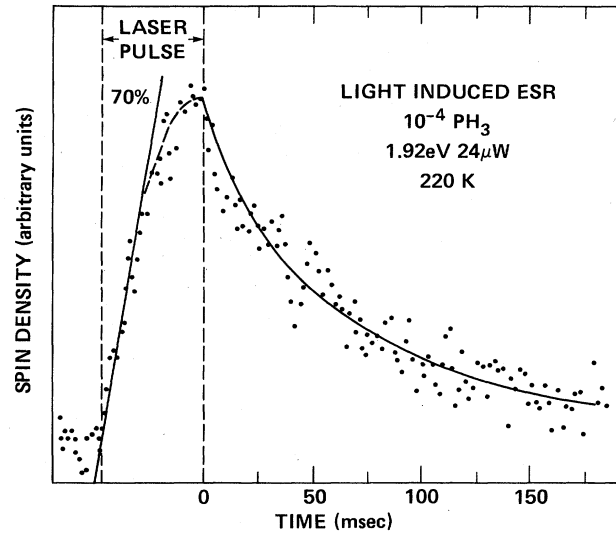


FIG. 7. Onset and decay of LESR for very weak illumination. The quantum efficiency of 70% for spin generation is measured from the linear onset of LESR.

The LESR decay times increase as the excitation intensity decreases (compare Figs. 6 and 7), indicative of a bimolecular process, just as was deduced from the luminescence. The steady-state LESR is strongly sublinear in the excitation density, again confirming the bimolecular recombination. (Note that luminescence is linear even for bimolecular recombination.) In addition, we have measured LESR with subgap excitation and found essentially identical results.

Another interesting aspect of LESR is the determination of what fraction of the recombination is being observed. We attempt this by measuring the quantum effi-

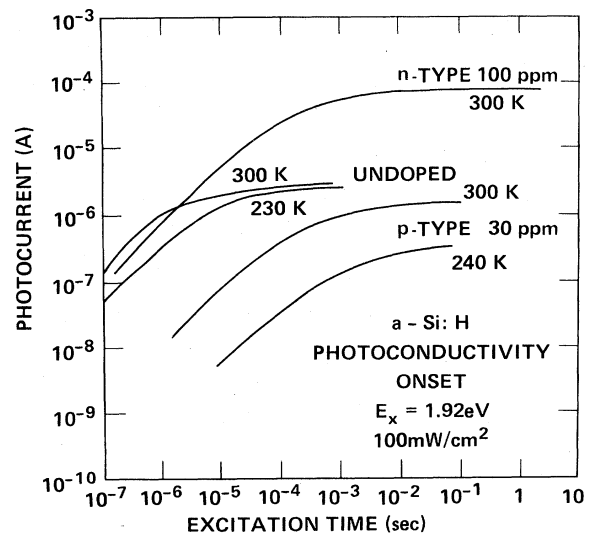


FIG. 8. Examples of the onset of gap-call photoconductivity for undoped and doped  $a$ -Si:H. The effective mobility is obtained from the linear onset, and an estimate of the recombination time is obtained from the saturation. Note the longer recombination times in the doped samples.

ciency  $\eta$  for generating the states observed in LESR. At times much less than the recombination times, LESR will increase linearly at a rate  $\eta G$ , where  $G$  is the absorbed photon flux. Figure 7 shows an example of the onset of LESR at the lowest excitation intensity measurable (so that the recombination times are long). The actual number of spins induced is calibrated using higher intensities, and from this data we deduce  $\eta \sim 70\%$ . This figure has an uncertainty of at least a factor of 2, both on account of signal-to-noise limitations as well as uncertainties in the various corrections needed (e.g., reflectivity, absorption, spin calibration, ESR saturation, etc.). Measurements of  $p$ -type material give similar values for the efficiency.

We therefore observe that LESR and luminescence have many common features, specifically that in doped samples the recombination is bimolecular, involves band-tail and dangling-bond states, and has decay times of order 1–10 msec. In addition, the quantum efficiency demonstrates that this recombination channel is at least a major contribution to the recombination, and probably the dominant process.

#### IV. RELATED MEASUREMENTS OF RECOMBINATION

Other measurements have been performed that explore recombination under comparable experimental conditions. One example is photoinduced absorption. Vardeny *et al.*<sup>8</sup> report that the decay in  $n$ -type  $\alpha$ -Si:H extends to  $\sim 1$  msec and is only weakly temperature dependent. They also deduce that the recombination is bimolecular, and analyze the results in terms of dispersive transport of one of the carriers.

Very similar conclusions have been reported from measurements of gap-cell photoconductivity in  $n$ -type samples.<sup>4,5</sup> Here we report our own photoconductivity data.

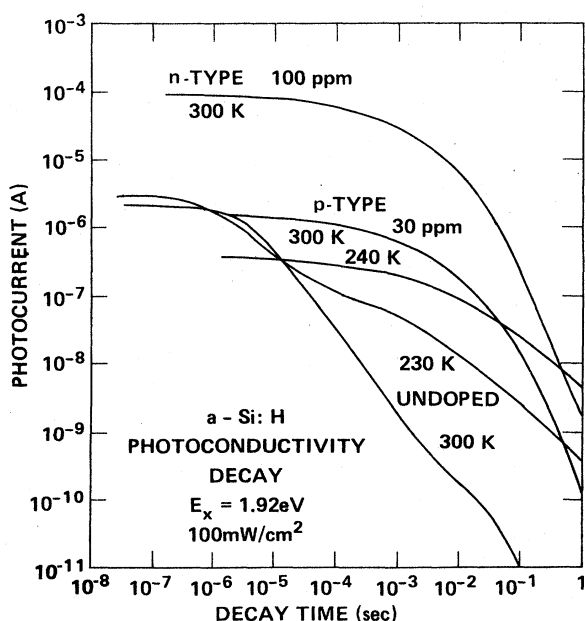


FIG. 9. Decay of photoconductivity for the same samples as in Fig. 8.

TABLE II. dc-conductivity activation energies ( $E_\sigma$ ), room-temperature drift mobilities ( $\mu$ ), and mobility-lifetime ( $\mu\tau$ ) products as obtained by gap-cell photoconductivity data.

	$E_\sigma$ (eV)	$\mu$ ( $\text{cm}^2/\text{V sec}$ )	$\mu\tau$ ( $\text{cm}^2/\text{V}$ )
Undoped	0.75	0.4	$6.9 \times 10^{-7}$
$10^{-4}$ $\text{PH}_3$	0.23	0.05	$2.2 \times 10^{-5}$
$3 \times 10^{-5}$ $\text{B}_2\text{H}_6$	0.67	$1.4 \times 10^{-3}$	$3.5 \times 10^{-7}$

For these measurements, evaporated Cr electrodes with gaps of  $175 \mu\text{m}$  were used. The excitation pulse length was typically 100 msec, at a repetition rate of 0.2 Hz. Other details of the measurements will be published elsewhere. Representative results for undoped,  $n$ -type, and  $p$ -type samples are shown in Figs. 8 and 9, which illustrate the onset and decay of the photoconductivity. The risetime for undoped  $\alpha$ -Si:H is on the order of  $10^{-6}$  sec and is only weakly temperature dependent. In both  $p$ - and  $n$ -type samples the risetime is much longer, about  $10^{-3}$  sec, and is more temperature dependent. These results again demonstrate the increase in response time in doped samples, as in the other experiments. The initial, linear portion of the rise curve is controlled by photogeneration, and hence is proportional to the carrier drift mobility. The undoped and  $n$ -type samples have a similar rate of rise and are both clearly controlled by electrons. The deduced drift mobility is about  $0.1 \text{ cm}^2/\text{V sec}$  at 300 K. In contrast, the  $p$ -type sample has a much lower photoresponse, giving a 300-K mobility of  $10^{-3} \text{ cm}^2/\text{V sec}$  and a stronger temperature dependence, clearly indicating hole transport. The uncertainty in these values is about a factor of 3 on account of errors in the measurement of the excitation density.

Figure 9 shows the decay of photocurrent from quasi-steady-state conditions after the light is turned off. The results are consistent with the rise-time data, and again the undoped sample shows the most rapid response. There is a slow component to the decay of the undoped sample which appears as a shoulder near  $10^{-3}$  sec at 300 K and at  $10^{-2}$  sec at 250 K. This structure is possibly due to long-lived holes, as the decay is similar to that in the  $p$ -type samples.

A summary of the dc-conductivity activation energies, room-temperature drift mobilities, and mobility-lifetime products is given in Table II.

#### V. DISCUSSION

Our previous model assigned the defect luminescence at 10 K to a transition between band-tail holes and negative dangling bonds.<sup>10</sup> The transition was assumed to be the same in both  $n$ - and  $p$ -type samples, which required that in  $p$ -type material substantial saturation of the defects occurred at low excitation intensities. This saturation, however, was never observed. The main evidence for this model was the similarity of the luminescence spectra and of the thermal quenching for the two types of doping. In the present data the defect transition is observable to much lower doping levels because of the higher measurement temperature. The data in Fig. 1 show that different

peaks are present for the two doping types, and that this difference extends down to the lowest doping level, and thus cannot be attributed to a shift in the band gap. We therefore conclude that, at least at 250–300 K, the transitions are different, and there are two other pieces of evidence to support this view. First, the light-induced ESR measurements show that at 250 K the defects are definitely not saturated at the typical excitation intensities used. This result and the linear intensity dependence of defect luminescence argue strongly against any model involving saturation. Second, the comparable luminescence efficiency observed with subgap excitation also cannot be understood in terms of saturation.

Although the previous model no longer holds, the present data do provide some additional evidence that the defect luminescence is indeed related to dangling-bond recombination. Time-of-flight experiments reveal that light doping results in fast trapping of minority carriers at charged dangling bonds.<sup>11</sup> The boron-doped samples used here are in fact from the same deposition as in that study. It is very appealing to attribute the quenching of the band-tail luminescence to the capture of minority carriers, and the defect luminescence to recombination through those defects. The fast minority-carrier trapping also explains the fast decay of the band-tail luminescence as seen in Fig. 5.

The new luminescence and ESR data therefore suggest the model shown in Fig. 10. This model uses the density of states deduced from our previous studies of dangling bonds.<sup>11</sup> Undoped samples contain a low density ( $10^{-15}$   $\text{cm}^{-3}$ ) of predominantly neutral defects, while doping increases the density of dangling bonds, which also become charged because of the shift of the Fermi energy.<sup>19</sup> Consider first the doped samples and above-gap excitation. Recombination occurs in two steps. The first is the capture of the minority carrier by a charged defect. This is expected to be a monomolecular process, and the evidence of transport data is that the capture rate is fast.<sup>11</sup> For example, with 10-ppm-boron doping the 300-K trapping time for electrons is about  $10^{-9}$  sec. The second step is the recombination of the majority carrier with the neutral defect. This will be bimolecular provided the excess carrier density is larger than the equilibrium carrier density. With subgap excitation the defects are directly excited,<sup>17</sup> so that recombination is a single bimolecular process cor-

responding to the second step described above. Since the luminescence has bimolecular characteristics and is the same for both types of excitation, we conclude that the radiative transition is the second step, as shown in Fig. 10. An analogous argument applies to *p*-type material, so that in each case the luminescence corresponds to the capture of the majority carrier into the neutral dangling bond.

In undoped samples there are four transitions to consider, of which two should be radiative and two nonradiative according to the above discussion (see Fig. 10). The position of the luminescence spectrum at 0.8 eV rather than 0.9 eV suggests that the dominant transition is the capture of electrons by neutral defects.

Another aspect of the luminescence that deserves comment is the low efficiency of the  $D_B$  and  $D_P$  transitions. We believe that the correct interpretation of this observation is that the capture of carriers into any dangling bond can proceed either radiatively or nonradiatively, and that the relative rates do not vary substantially from site to site. Hence, luminescence will be observed from transitions at any dangling bond, but the efficiency is reduced by the low statistical probability that any particular event is radiative. The alternative possibility is that the luminescence is internally efficient but originates from a small subset of recombination centers unrelated to the dominant mechanism. Our choice of model is based on the two conclusions, namely that near 300 K the dominant recombination is through dangling bonds, and that the luminescence also occurs at the dangling bonds. Clear evidence for the first point is given by the LESR data discussed above. Evidence for the second point is mostly circumstantial, but plentiful enough to be convincing.<sup>1,10</sup>

The thermal quenching of both defect peaks is known to be very similar.<sup>10,18</sup> Previously we used this fact as evidence that the transition was the same in *n*- and *p*-type *a*-Si:H, a model that our present data now show to be incorrect. It remains, therefore, to account for the quenching within the present model. Our earlier interpretation was that the quenching was caused by excitation to the band edge followed by a competing nonradiative process. However, there is no such competing process, if the recombination is essentially all through the dangling bonds. We therefore suggest that the thermal quenching represents the change in the ratio of radiative and nonradiative rates at a particular defect. Presently we do not have a detailed model for the nonradiative process, which is discussed further in Sec. VA. However, it seems reasonable to suppose that its temperature dependence is similar for capture of both electrons and holes.

The preceding results present a rather clear and consistent picture of recombination based on the model of Fig. 10. Measurements of luminescence and LESR, as well as induced-absorption, photoconductivity, and time-of-flight experiments, all are in qualitative agreement. In addition, given the presence of gap states originating from dangling bonds, the proposed model is the most obvious one, being the Shockley-Read mechanism.

However, there are many details of the recombination yet to be resolved. The remainder of the discussion will focus on two of these, namely the deep trapping mechanism and the doping dependence of the recombination

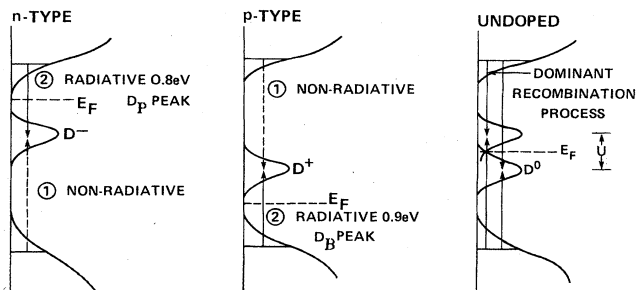


FIG. 10. Schematic density of states used to explain the recombination and luminescence in doped and undoped *a*-Si:H. The defect levels, the Fermi energy, and the various transitions are shown.

rates. As we shall see, further work is needed to resolve these questions.

#### A. Defect energy levels and trapping mechanisms

If the defect luminescence is a transition to a neutral dangling bond, as indicated in Fig. 10, then the luminescence energy provides information about the trap depth. To obtain this information we must first discuss some small corrections concerning the normalization of the spectrum. As in our previous measurements, the data are normalized to give the energy density of the luminescence. In order to facilitate comparison with other data, the results should be corrected for the energy per emitted photon. This results in a shift of the peak to lower energy by  $S^2/2E_0$ , where  $S$  is the Gaussian width of the peak and  $E_0$  is the peak energy. For the defect peaks the correction is about 0.03 eV, so that at 250 K the peak energies are 0.78 and 0.88 eV. Furthermore, in order to compare these data with other data taken at room temperature, there is a further correction of  $-0.02$  eV for the temperature shift of the luminescence energy. The experimental uncertainty in the peak energy is estimated to be about 0.03 eV, but is hard to determine since it is probably dominated by errors in the normalization procedure.

Thus, the 300-K capture of an electron by  $D^0$  gives weak luminescence at about 0.75 eV in *n*-type material and 0.85 eV in *p*-type material. Deep-level transient-spectroscopy (DLTS) data show the energy level of  $D^0$  to be 0.8–0.9 eV below the conduction-band mobility edge.<sup>20,21</sup> The spread in the energy includes an uncertainty of about 0.05 eV originating from the estimate of the prefactor in the thermal excitation rate. The equivalent trap depth for holes is as yet unknown. A comparison of the DLTS peak (from Ref. 20) and the corrected luminescence spectrum in Fig. 11 shows that the bands are indeed of comparable shape and position. The defect correlation

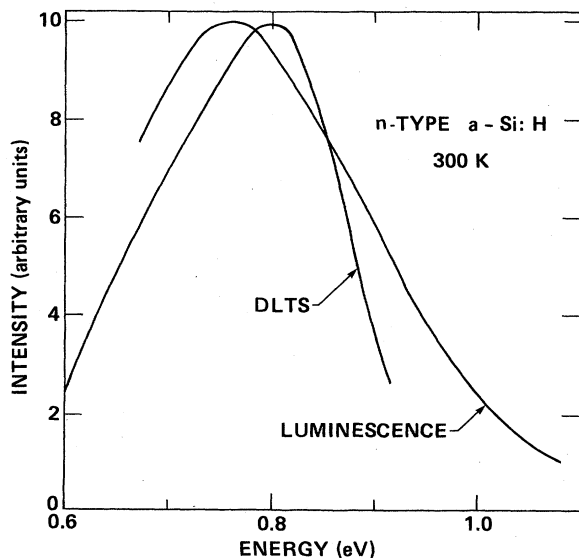


FIG. 11. Comparison of the DLTS band (Ref. 20) and the luminescence spectrum of *n*-type *a*-Si:H. According to the present model, both experiments measure the same transition.

energy has been estimated to be  $\sim 0.3$  eV with an uncertainty of  $\sim 0.1$  eV.<sup>22</sup> Both luminescence transitions may have Stokes shifts arising from distortion energies denoted by  $W_N$  and  $W_P$  for *n*- and *p*-type samples. We also assume for the moment that the initial state of the transition is below the mobility edge by an energy  $E_N$  and  $E_P$  in the two cases. Hence, if the separation of the mobility edges is  $E_G$ , then

$$\begin{aligned} E_G &= 0.75 + 0.85 + 0.3 + W_N + W_P + E_N + E_P \\ &= 1.9 + W_N + W_P + E_N + E_P, \end{aligned}$$

and in regard to the DLTS data,

$$0.8 = 0.75 + W_N + E_N.$$

Since the mobility gap is believed to be no larger than 2.0 eV,<sup>21</sup> it is evident that  $W_N$ ,  $W_P$ ,  $E_N$ , and  $E_P$  are all small. This leads us to two conclusions, namely that the defect luminescence represents a transition from the mobility edge or very near it, and that the Stokes shift is small. Recent analysis suggests that trapping at dangling bonds does indeed occur from close to the mobility edge.<sup>23</sup> On the other hand, the band-tail luminescence evidently occurs from deeper tail states. The difference can be seen, for example, from the temperature dependence of the luminescence energy, which follows the band gap for the defect peaks,<sup>10</sup> but is much stronger for the band-tail peak.<sup>15</sup> We suggest that the distinction arises because capture at the defect is largely nonradiative, whereas the band-tail transition is radiative. The band-tail transition is determined by the competing process of thermal excitation and diffusion away of weakly bound carriers, so that *only* the deeper states give luminescence. On the other hand, the defect transition reflects the dominant trapping process, which is from near the mobility edge. A schematic energy-level diagram of our recombination model is shown in Fig. 12.

The small distortion energy, apparently no greater than about 0.05 eV, compares with a larger estimated value of 0.2–0.25 eV for the band-tail transition.<sup>1,24</sup> It is unusual for a lower-energy transition to have a smaller distortion, but in this case it can perhaps be understood. The distortion energy of the band-tail transition has been attributed

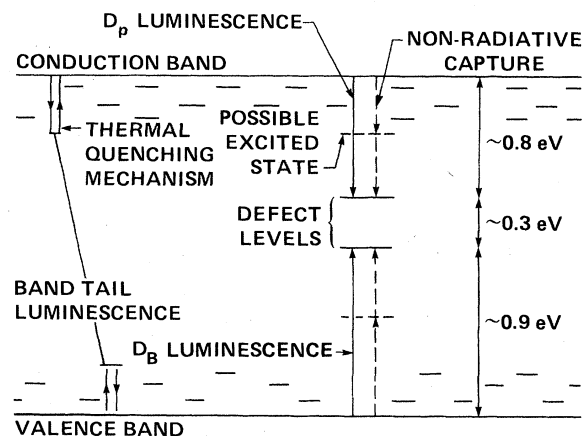


FIG. 12. Schematic diagram showing the energy levels and our model for the luminescence transitions.

to the relatively deep holes,<sup>15</sup> and we argue that the removal of an electron from a bond will weaken the bond and relax the local network. Band-tail electrons apparently have a much smaller distortion energy, possibly because they are less strongly localized than holes. The initial state of the defect transition is evidently close to the mobility edge, and therefore also weakly localized, and thus should not result in much relaxation. The final state of the transition is the dangling bond. Since this state is nonbonding, a change in electron occupancy may not result in significant relaxation of the lattice. In fact, calculations [J. Northrup (private communication)] reveal that there is indeed very little relaxation of a dangling bond between its different charge states. It is possible that the  $D_B$  transition has a larger distortion energy than the  $D_P$  transition because the former transition involves holes. The broader spectrum is consistent with this suggestion.

The small distortion energy has implications for the possible recombination mechanisms. Our explanation of the low efficiency of defect luminescence is that most of the electrons recombine at dangling bonds nonradiatively. There is a well-established criterion for multiphonon transitions, namely that the nonradiative rate only exceeds the radiative rate when the distortion energy is half the luminescence energy.<sup>25</sup> The present case requires  $W_N > 0.35$  eV, which is too large to be compatible with the other energy-level measurements. An Auger transition also does not seem to be a possibility within the present model because there is insufficient energy to excite a second carrier.

A related point concerns the magnitude of the dangling-bond capture cross section and its temperature dependence. According to the theory of multiphonon transitions,<sup>26</sup> a cross section of order  $10^{-15}$  cm<sup>2</sup> with a weak temperature dependence, as observed by time-of-flight measurements in *a*-Si:H,<sup>23</sup> requires the distortion energy to be of similar magnitude as the trap depth, and therefore about 0.8 eV. Again, this value is much larger than the measured one.

The multiphonon model therefore does not seem to apply immediately to *a*-Si:H. Assuming that the theory of such transitions is essentially correct, we consider two alternative explanations. One possibility is that there is a distribution of dangling bonds such that the luminescence occurs at only a small fraction of states. For example, the deepest states might be expected to have a larger luminescence efficiency because the competing multiphonon rate is reduced. In addition, the distortion energies may have a wide distribution, not necessarily corresponding to the distribution of defect energies. In this case the luminescence would tend to originate from the states with the smallest distortion energy, and the large capture cross sections from states with a large distortion energy.

The alternative explanation is that there may be intermediate states in the defect transition. If these were present, then the capture cross section could be explained by a cascade process without requiring a large distortion energy, because the multiphonon rate depends exponentially on the energy released in the capture process.

Although the dangling bonds are undoubtedly distributed in energy, as seen from the DLTS data<sup>20</sup> in Fig. 11,

and probably also in the size of their distortion, it seems unlikely to us that the distribution is large enough to be the only explanation. We believe that the presence of intermediate states is indicated, being the only obvious alternative, and this possibility should be explored further. In this case the luminescence would correspond to direct capture from the mobility edge, whereas the recombination usually goes through the intermediate state, as indicated in Fig. 12. Little is known about whether or not the dangling bond has excited states in the gap. One possibility is that the antibonding states of the back bonds are brought down into the gap because of the lower coordination.<sup>27</sup> An alternative possibility is that the dangling bond is associated with a small void of sufficient size to localize an excited state. The most obvious way to observe such states experimentally is by optical absorption at low energy. The transition from ground to excited state would have the characteristic feature of not exciting photoconductivity, since in order for the mechanism to operate, the return to the ground state must be more probable than release into the band. Nonphotoconductive absorption is indeed observed below about 0.8 eV in *a*-Si:H.<sup>28</sup> However, at present this has not been studied sufficiently to draw any firm conclusions as to its origin.

## B. Recombination rates

The decay measurements provide specific data about the recombination rates, and it is of interest to compare the various experiments. The recombination in doped samples is governed by bimolecular kinetics, and it must be recognized that the details of the decay may be governed by dispersive transport. Nevertheless, the steady-state density of excited carriers  $N_0$  is given by  $G\tau$ , where  $G$  is the generation rate and  $\tau$  is an average lifetime. The initial decay (e.g., the time for the density to fall by a factor of 2) is a measure of  $\tau$ .

We have already pointed out that luminescence measures  $dN(t)/dt$  rather than  $N(t)$ , which results in a faster decay. Light-induced ESR, photoconductivity, and induced absorption are therefore more appropriate measures of the recombination, and each gives decay times of order  $10^{-3}$  sec in *n*-type samples. According to our model, the rate-limiting recombination is the bimolecular capture of electrons into holes trapped at neutral dangling bonds. For capture of electrons into neutral dangling bonds in undoped samples it is found, from time-of-flight data, that  $\mu\tau N_s = 2.5 \times 10^8$  cm<sup>-1</sup> V<sup>-1</sup>, where  $\mu$  is the electron drift mobility,  $\tau$  is the trapping time, and  $N_s$  is the density of defects.<sup>11</sup> This quantity depends only slightly on temperature. In a typical LESR experiment, such as in Fig. 6, the steady-state spin density is  $\sim 3 \times 10^{16}$  cm<sup>-3</sup>. Assuming the electron mobility to be 0.1 cm<sup>2</sup>/V sec at 250 K yields  $\tau \sim 10^{-7}$  sec, which is 4 orders of magnitude less than the observed times. A similar estimate for holes gives a longer lifetime of about  $10^{-5}$  sec because the hole mobility is much smaller; this value, however, is also much less than the measured ones. The decay in undoped samples is much faster (Figs. 3, 6, and 9) and, therefore, more in line with the time-of-flight data. Nevertheless, the LESR decay is substantially longer than expected, al-



though the photoconductivity data agree well with the time-of-flight data.

It could be argued that the effective mobility is lower than that given by time-of-flight data because of dispersive-transport effects and band tailing. During prolonged illumination the population of deep band-tail states will build up and lead to an apparent reduction in the mobility of those carriers. The type of power-law response observed in the decay has been analyzed in terms of the dispersive process involving band-tail states.<sup>5,8</sup> Although this seems to be a plausible explanation in undoped samples, it is not so in *n*-type material. For example, in *n*-type samples at doping levels above 10 ppm, the Fermi energy is only  $\sim 0.2$  eV below the conduction band and electrons cannot thermalize to lower energy. The release time is  $\omega_0 \exp(-E_F/kT)$ , which is about  $10^{-8}$  sec. Hence, electrons at the Fermi energy come into thermal equilibrium with the band very quickly, and an explanation of the long decay times in terms of dispersive transport is not possible. Indeed, even in the absence of excess carriers the electrons equilibrating with the Fermi energy will contribute to the recombination with a rate given by

$$dN_0/dt = nN_0\sigma v = N_0/\tau,$$

where  $n$  is the free-carrier density,  $\sigma$  is the capture cross section, and  $v$  is the free-carrier thermal velocity.  $N_0$  is the density of trapped holes (neutral dangling bonds), and we assume that trapping occurs only from the mobility edge. The dark conductivity  $\sigma_D$  is given by  $n e \mu_0$ , where  $\mu_0$  is the free-carrier mobility, so that

$$\tau^{-1} = \sigma v \sigma_D / e \mu_0.$$

Taking measured values for 100-ppm doping,  $\sigma_D = 10^{-3} \Omega^{-1} \text{cm}^{-1}$ ,  $\mu_0 = 10 \text{ cm}^2/\text{V sec}$ ,  $v = 10^7 \text{ cm/sec}$ , and  $\tau = 10^{-3} \text{ sec}$ , then  $\sigma \sim 10^{-19} \text{ cm}^2$ . This value compares with  $\sigma \sim 10^{-15} \text{ cm}^2$  obtained for neutral dangling bonds in undoped material using the same values for  $\mu_0$  and  $v$ .

Our results therefore show that the apparent trapping rate of electrons at  $D^0$  is lower in *n*-type *a*-Si:H compared to undoped material by several orders of magnitude. There seem to be three possible mechanisms that can explain this result.

(1) The capture cross section could indeed be less than that in undoped material because different defects are involved. Doping is known to introduce defects,<sup>19</sup> so it is clearly possible that these have a different structure from those in undoped samples. Indeed, a defect-impurity pair has been suggested previously by us.<sup>29</sup> On the other hand, the required change in  $\sigma$  of a factor of  $10^4$  or more suggests a grossly different defect structure. However, the ESR and luminescence spectra of the defect are essentially indistinguishable in doped and undoped material, indicating that both the defect structure and its energy level are not substantially changed.<sup>19</sup>

(2) Electrons may be prevented from reaching neutral defects by some inhomogeneity in the doped samples. One possibility is long-range potential fluctuations introduced by the Coulomb interaction of the distribution of charged defects and dopants. After excitation, holes will tend to move to defects in just those regions excluded by electrons, making recombination less probable. This

model can readily explain why the recombination times become progressively longer with increased doping since the density of charges increases. Another attractive feature is that potential fluctuations have been suggested to account for the difference between thermopower and conductivity data,<sup>30</sup> and for the Meyer-Neldel rule, in which the conductivity prefactor depends on the position of the Fermi energy.<sup>31</sup> Within this model there is a potential barrier to impede recombination so that the decay time might be expected to be activated, but this is not observed experimentally. However, a distribution in barrier heights would weaken any temperature dependence. In addition, subgap excitation should be less selective of fluctuations that exclude electrons, and yet the decay data are essentially the same as for above-gap excitation.

(3) The capture cross section may have a broad distribution that is sampled differently by different experiments. There have been several occasions when such a distribution has led to apparent inconsistencies,<sup>3</sup> and this possibility definitely exists in the present case. For example, the steady-state density of excited states is  $G\tau$  and thus will be dominated by those states with the largest  $\tau$ . In undoped samples, the time-of-flight experiment measures the behavior of a few carriers in the presence of many defects. In this case, recombination will be dominated by those defects with the smallest  $\tau$ . Hence, a distribution of cross sections spanning three or more decades could account for some of the results. In fact, the nonexponential form of the decay indicates that there may be a distribution of recombination times covering this sort of range.

It is possible that each of these mechanisms contributes to some extent. At present we do not have the information to make any further conclusions. In particular, we need a better understanding of whether potential fluctuations exist in *a*-Si:H, measurements of the distribution of capture rates, either by DLTS or time-of-flight measurements, and more details about how the drift mobility is influenced by doping.

## VI. SUMMARY AND CONCLUSIONS

We have measured luminescence, LESR, and photoconductivity of *a*-Si:H in the temperature range 200–300 K. The low-energy luminescence transition is at a different energy in lightly doped *n*- and *p*-type material, demonstrating that two distinct transitions occur. Transient data reveal that there is a distribution of decay times, with an intensity dependence indicative of bimolecular recombination. The quantum efficiency of inducing LESR is measured and shows that dangling bonds dominate the recombination. The observed decay times of luminescence, LESR, and photoconductivity, and their dependence on intensity and doping, are all similar when allowances are made for the different experimental details.

Our conclusions from these results are as follows:

(1) The previous model<sup>10</sup> we proposed to explain the low-energy, defect-related luminescence transition is incorrect, at least for temperatures above 200 K. We now propose that the luminescence, in both *n*- and *p*-type material, is the capture of majority carriers from near the mobility edge into neutral dangling bonds. Consideration of the energy levels leads us to conclude that the transi-

tion occurs with only a small Stokes shift.

(2) From the rise time of light-induced ESR we conclude that recombination through dangling-bond levels is the dominant recombination mechanism. The data are consistent with this process accounting for virtually all of the recombination, although the experimental uncertainty in the result is substantial.

(3) A single multiphonon transition does not seem able to account for the capture of carriers into dangling bonds. Instead, we propose that a cascade capture mechanism occurs, although we cannot yet identify the excited states involved. However, there is some evidence for the existence of such states.

(4) The recombination times in doped samples are much longer than in undoped samples. Analysis of the data

shows that these times are apparently incompatible with the trapping rates deduced for undoped *a*-Si:H. We discuss the possible reasons for the difference, but without reaching any firm conclusions. However, we believe that, particularly in *n*-type *a*-Si:H, the decay data cannot be explained by a dispersive-transport mechanism.

#### ACKNOWLEDGMENTS

Helpful discussions with D. J. Chadi, G. H. Döhler, W. B. Jackson, and N. M. Johnson are gratefully acknowledged. We also benefited from the technical assistance of R. Thompson and J. Zesch. This research was partially supported by the Solar Energy Research Institute under Contract No. XB-3-03112-1.

- <sup>1</sup>R. A. Street, *Adv. Phys.* **30**, 593 (1981), and references therein.
- <sup>2</sup>D. K. Biegelsen, *Solar Cells* **2**, 421 (1980).
- <sup>3</sup>R. A. Street and D. K. Biegelsen, *Solid State Commun.* **44**, 501 (1982).
- <sup>4</sup>D. A. Anderson and W. E. Spear, *Philos. Mag.* **36**, 695 (1977).
- <sup>5</sup>J. M. Hvam and M. H. Brodsky, *Phys. Rev. Lett.* **46**, 371 (1981).
- <sup>6</sup>C. R. Wronski and R. E. Daniel, *Phys. Rev. B* **23**, 794 (1981).
- <sup>7</sup>P. D. Persans, *Philos. Mag. B* **46**, 435 (1982).
- <sup>8</sup>Z. Vardeny, P. O'Connor, S. Ray, and J. Tauc, *Phys. Rev. Lett.* **44**, 1267 (1980).
- <sup>9</sup>W. B. Jackson and R. J. Nemanich, in *Proceedings of the 10th International Conference on Amorphous and Liquid Semiconductors*, edited by K. Tanaka and T. Shimizu (North-Holland, Amsterdam, 1983), p. 353.
- <sup>10</sup>R. A. Street, *Phys. Rev. B* **21**, 5775 (1980).
- <sup>11</sup>R. A. Street, J. C. Zesch, and M. J. Thompson, *Appl. Phys. Lett.* **43**, 672 (1983).
- <sup>12</sup>I. Solomon, T. Dietl, and D. Kaplan, *J. Phys. (Paris)* **39**, 1241 (1978).
- <sup>13</sup>W. B. Jackson, R. A. Street, and M. J. Thompson, *Solid State Commun.* **47**, 435 (1983).
- <sup>14</sup>R. A. Street, J. C. Knights, and D. K. Biegelsen, *Phys. Rev. B* **18**, 1880 (1978).
- <sup>15</sup>C. Tsang and R. A. Street, *Phys. Rev. B* **19**, 3027 (1979).
- <sup>16</sup>R. A. Street, *Phys. Rev. B* **23**, 861 (1981).
- <sup>17</sup>W. B. Jackson and N. M. Amer, *Phys. Rev. B* **25**, 5559 (1982).
- <sup>18</sup>R. A. Street and D. K. Biegelsen, *Solid State Commun.* **33**, 1159 (1980).
- <sup>19</sup>R. A. Street, D. K. Biegelsen, and J. C. Knights, *Phys. Rev. B* **24**, 969 (1981).
- <sup>20</sup>N. M. Johnson, *Appl. Phys. Lett.* **42**, 981 (1983).
- <sup>21</sup>D. V. Lang, J. D. Cohen, and J. P. Harbison, *Phys. Rev. B* **25**, 5285 (1982).
- <sup>22</sup>W. B. Jackson, *Solid State Commun.* **22**, 133 (1982).
- <sup>23</sup>R. A. Street, *Philos. Mag. B* **49**, L15 (1984).
- <sup>24</sup>R. A. Street, *Philos. Mag. B* **37**, 35 (1978).
- <sup>25</sup>D. L. Dexter, C. C. Klich, and G. A. Russell, *Phys. Rev.* **100**, 603 (1955).
- <sup>26</sup>C. H. Henry and D. V. Lang, *Phys. Rev. B* **15**, 989 (1977).
- <sup>27</sup>D. J. Chadi (private communication).
- <sup>28</sup>W. B. Jackson, R. J. Nemanich, and N. M. Amer, *Phys. Rev. B* **27**, 4861 (1983).
- <sup>29</sup>D. K. Biegelsen, R. A. Street, and J. C. Knights, in *Tetrahedrally Bonded Amorphous Semiconductors (Carefree, Arizona)*, a Topical Conference on Tetrahedrally Bonded Amorphous Semiconductors, edited by R. A. Street, D. K. Biegelsen, and J. C. Knights (AIP, New York, 1981), p. 166.
- <sup>30</sup>H. Overhof and W. Beyer, *Philos. Mag. B* **43**, 433 (1981).
- <sup>31</sup>H. Overhof and W. Beyer, *Philos. Mag. B* **47**, 377 (1983).